

Crossover of angular dependent magnetoresistance with the metal-insulator transition in colossal magnetoresistive manganite films

Y. Z. Chen,^{1,2,a)} J. R. Sun,^{1,b)} T. Y. Zhao,¹ J. Wang,¹ Z. H. Wang,¹ B. G. Shen,¹ and N. Pryds²

¹State Key Laboratory of Magnetism, Institute of Physics and Beijing National Laboratory for Condensed Matter Physics, Chinese Academy of Sciences, Beijing 100190, People's Republic of China

²Fuel Cells and Solid State Chemistry Division, Risø National Laboratory for Sustainable Energy, Technical University of Denmark, Roskilde 4000, Denmark

(Received 25 August 2009; accepted 7 September 2009; published online 1 October 2009)

The temperature and magnetic field dependence of angular dependent magnetoresistance (AMR) along two orthogonal directions ([100] and $[0\bar{1}1]$) was investigated in a charge-orbital-ordered $\text{Sm}_{0.5}\text{Ca}_{0.5}\text{MnO}_3$ (SCMO) film grown on (011)-oriented SrTiO_3 substrates. A dramatic decrease of AMR magnitude in both directions was observed with the appearance of magnetic-field-induced metal-insulator transition, which further led to a sign crossover in the AMR effect. The AMR crossover may give a direct evidence of the drastic modification of electronic structure or possible orbital reconstruction with the magnetic-destruction of charge/orbital ordering in SCMO films. © 2009 American Institute of Physics. [doi:10.1063/1.3240407]

The most striking aspect of physics for manganites is the occurrence of a magnetic-field-induced insulator-to-metal transition—colossal magnetoresistance (CMR) effect.¹ Besides magnetic fields, the metal-insulator transition (MIT) could be initiated by a number of other external stimuli, such as temperature, electric field, pressure, and irradiation with light, which exhibits intriguing applications potential in multifunctional oxide electronic devices.¹ The huge change in conductivity could be attributed to melting of long-range and/or short-range charge/orbital ordering (COO), a percolation transition, or a sliding charge-density wave.² However, no consensus in the microscopic mechanism of the MIT has been reached yet.

The competition between a ferromagnetic metallic state and a paramagnetic insulating phase underlies the CMR phenomenon. This phase competition appears due to the natural coupling between magnetism and orbital ordering. In fact, the spin-orbit coupling is also at the origin of the anisotropic magnetoresistance in ferromagnets.^{3,4} Due to the strong coupling between the charge, orbital, spin, and lattice degrees of freedom, manganites present anomalous behavior in their anisotropic magnetoresistance or the angular dependent magnetoresistance (AMR) compared to the conventional ferromagnetic alloys.^{5–11} For example, the AMR effect could persist up to the paramagnetic region. In particular, a peak in AMR is always observed near the Curie temperature T_C of ferromagnetic manganites,^{5–9} where a spontaneous MIT together with a Jahn–Teller (JT) distortion occurs. Although it could not satisfactorily explained by the most traditional explanation of AMR as that in ferromagnetic metals appealing on the spin-orbit coupling and the anisotropic scattering rate of charge carriers, such AMR behavior seems to exhibit intimate correlation with JT distortion. Moreover, significant adjustments in the AMR, even a AMR sign change or crossover, have been observed in ultrathin $\text{Pr}_{0.67}\text{Sr}_{0.33}\text{MnO}_3$ (Ref. 10) and $\text{La}_{0.65}\text{Ca}_{0.35}\text{MnO}_3$ (Ref. 5) films, where the strain-

selected e_g orbital occupation prevails.^{12,13} These results clearly indicate an important role of lattice and orbital effect in AMR of manganites. For charge-orbital-ordered manganites, the CMR effect is much larger and is always accompanied with a magnetic-field-induced MIT, during which a ferromagnetic metal generally takes place the insulating COO state and orbital reconstruction occurs. Thus, it should be rather interesting to investigate the AMR effect in COO manganites with the evolution of the magnetic-field-induced MIT. In this letter, a dramatic crossover in the AMR effect due to the collapse of COO is observed, which further indicates the close relation of the AMR abnormality and the MIT. The underlying mechanism is also discussed.

The SCMO films were grown on (011)-oriented SrTiO_3 substrates by pulsed laser deposition. The film thickness was ~ 60 nm. The high quality of the films was confirmed by x-ray diffraction and reciprocal space maps measurements.¹⁴ Magnetotransport properties along the [100] and $[0\bar{1}1]$ directions, ρ_{100} and $\rho_{0\bar{1}1}$, respectively, were measured using the four-terminal method in a bridge-shaped sample patterned by the conventional photolithography and chemical etching technique, which showed the dimensions of 0.1 mm in width and 0.4 mm in length. For AMR measurements, the magnetic field was rotated in the (011) plane to prevent the demagnetization effect and the Hall effect signals, which was performed in a Quantum Design physical property measurement system (PPMS-14h). The AMR effect was deduced from the total magnetoresistance data by subtracting the overwhelming CMR contributions.

No obvious AMR angular dependence $[\text{AMR}(\theta)]$ is detected at a magnetic field $\mu_0 H < 6$ T in the whole temperature range (2–300 K) for the nonferromagnetic SCMO films. Such situation persists even for the magnetic field up to 14 T for $T > T_{\text{CO}}$ ($T_{\text{CO}} \approx 235$ K, the charge ordering temperature). However, $\text{AMR}(\theta)$ oscillations in both ρ_{100} and $\rho_{0\bar{1}1}$ appear once the COO forms and the $\mu_0 H$ is up to 6 T. Figures 1(a) and 1(b) show the linear (upper) and polar (lower) plots of the $\text{AMR}(\theta)$ oscillations in ρ_{100} and $\rho_{0\bar{1}1}$, respectively, at 150 K under different magnetic field. Here, $\text{AMR}(\theta) = (\rho_\theta$

^{a)}Electronic mail: yunc@risoe.dtu.dk.

^{b)}Electronic mail: jrsun@g203.iphy.ac.cn.

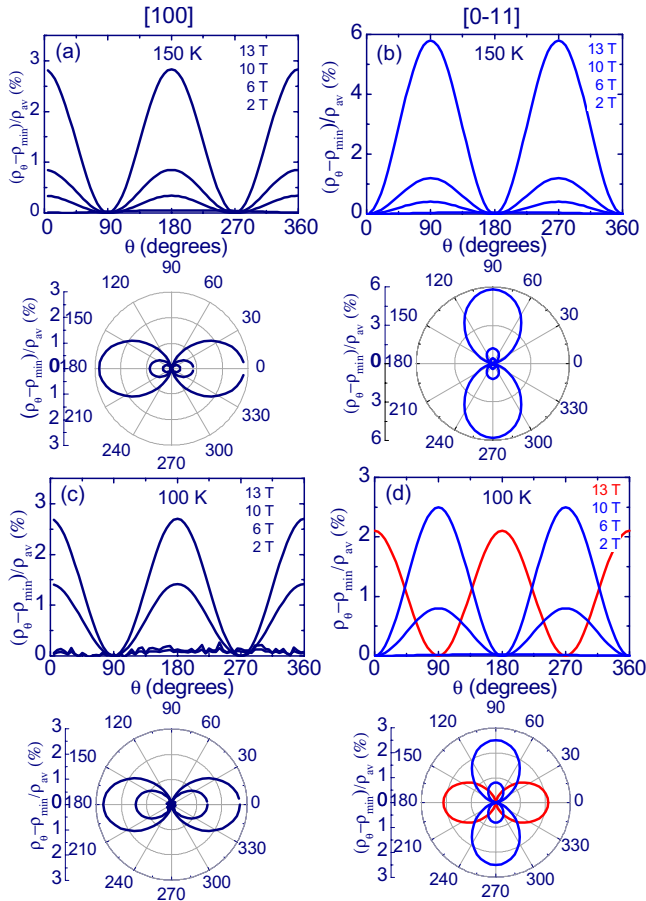


FIG. 1. (Color online) [(a)–(d)] Linear (upper) and polar (lower) plots of AMR oscillations, $(\rho_\theta - \rho_{\min})/\rho_{\text{av}}$, along both $[100]$ and $[0\bar{1}1]$ directions at 100 K and 150 K under different magnetic field.

$-\rho_{\min})/\rho_{\text{av}}$, ρ_{\min} , and ρ_{av} are the minimum and average resistivity, respectively, among the angular dependent resistivities. It is interesting to note that $\text{AMR}(\theta)$ shows $\cos^2 \theta$ dependence along $[100]$ direction, while $\sin^2 \theta$ dependence along $[0\bar{1}1]$ direction, which is distinctly opposite to the $\text{AMR}(\theta)$ observed in $\text{La}_{0.95}\text{Ag}_{0.05}\text{MnO}_3$ films with a ferromagnetic metallic state.⁶ As also shown in the figures, further increasing magnetic field enhances the $\text{AMR}(\theta)$ amplitude significantly. More interestingly, with decreasing temperature, a crossover of $\text{AMR}(\theta)$ from $\sin^2 \theta$ to $\cos^2 \theta$ dependence is observed in $\rho_{0\bar{1}1}$ for $\mu_0 H > 10$ T in $80 \text{ K} < T < 120$ K, while the $\cos^2 \theta$ -dependent $\text{AMR}(\theta)$ remains for ρ_{100} as illustrated in Figs. 1(c) and 1(d) ($T = 100$ K). When $T < 80$ K, another crossover of $\text{AMR}(\theta)$ from $\cos^2 \theta$ to $\sin^2 \theta$ is also observed in ρ_{100} . As a result, the $\text{AMR}(\theta)$ oscillations becomes similar to that of ferromagnetic metallic $\text{La}_{0.95}\text{Ag}_{0.05}\text{MnO}_3$ films,⁶ when $T < 80$ K and $\mu_0 H > 10$ T.

Figure 2 displays a typical temperature dependent $\text{AMR}(\theta)$ evolution in ρ_{100} and $\rho_{0\bar{1}1}$ under 13 T during cooling. The corresponding temperature dependent resistivities and AMR values are shown in Figs. 3(a) and 3(b), respectively. Here, the AMR value is obtained from the form of $(\rho_{\parallel} - \rho_{\perp})/\rho_{\text{av}}$, where ρ_{\parallel} and ρ_{\perp} are the resistivities with the current parallel ($\theta = 0^\circ$) and perpendicular ($\theta = 90^\circ$) to the magnetization, respectively. As shown in Fig. 3(a), the SCMO film shows a quicker increase of the resistivity upon decreasing temperature to T_{CO} due to the formation of COO,

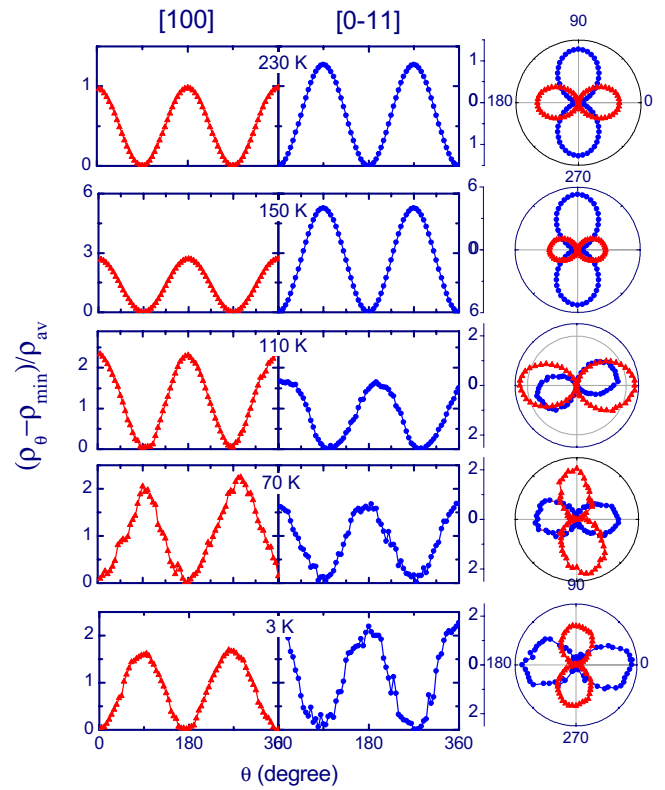


FIG. 2. (Color online) Linear (left) and polar (right) plots of temperature dependent evolution of AMR oscillations, $(\rho_\theta - \rho_{\min})/\rho_{\text{av}}$, along both $[100]$ and $[0\bar{1}1]$ directions under a field of 13 T.

where the collective JT distortion of the MnO_6 octahedron occurs and further evolves with decreasing temperature. In addition, the film exhibits a large transport anisotropy of $\rho_{100}/\rho_{0\bar{1}1} \approx 10$ at room temperature due to the strain effect.¹⁴ The anisotropic strain also leads to a significant different response of ρ_{100} and $\rho_{0\bar{1}1}$ with respect to external magnetic fields, for example a giant CMR anisotropy of larger than 10^3

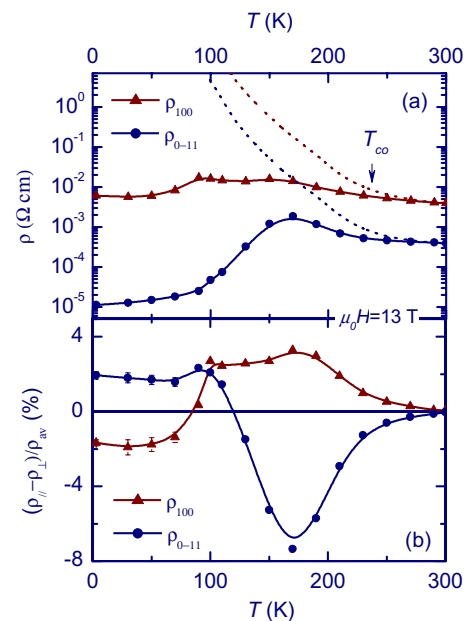


FIG. 3. (Color online) (a) The temperature dependent resistivities ρ_{100} and $\rho_{0\bar{1}1}$ under 0 T (dotted line) and 13 T. (b) The temperature dependent AMR effect under 13 T along both $[100]$ and $[0\bar{1}1]$ directions.

is obtained under a field of 13 T [Fig. 3(a)]. As shown in Fig. 3(b) and as mentioned previously, both AMR effects in ρ_{100} and $\rho_{0\bar{1}1}$ appear at $T=T_{CO}$. Meanwhile, the AMR magnitudes increase fast with further decreasing temperature. However, AMR turns to decrease with decreasing temperature when $T < 170$ K, which is followed by the AMR(θ) crossover at 120 K in $\rho_{0\bar{1}1}$ and near 80 K in ρ_{100} . Below 80 K, where “metallic” conducting behavior appears in both directions [Fig. 3(a)], the AMR exhibits little temperature dependence. Additionally, the value of $\rho_{0\bar{1}1}$ (with maximum of 7.3%) is essentially larger than that of ρ_{100} (with maximum of 3.3%) in the whole temperature range, which has also been observed in $\text{La}_{2/3}\text{Ca}_{1/3}\text{MnO}_3$ films.⁹ The most striking feature in the figures is the occurrence of the distinct AMR decrease [Fig. 3(b)] once the magnetic-induced metallic conducting behavior begins to play a role [Fig. 3(a)]. The results clearly demonstrate that the magnetic-field-induced MIT also make a dramatic signature in AMR in COO manganites, besides the AMR peak in the vicinity of MIT for ferromagnetic manganites. In addition, the decrease of AMR magnitude and its sign change in the field-induced conducting region should indicate an opposite AMR(θ) behavior between the COO state and the field-induced metallic one, while the latter exhibits a similar behavior as the ferromagnetic $\text{La}_{0.95}\text{Ag}_{0.05}\text{MnO}_3$.⁶

Generally, the AMR mainly arises from the convoluted nature of the Fermi surface or the scattering anisotropies due to the spin-orbit interaction. Considering the disappearance of the H^2 -dependent magnetoresistance and the small $\omega_c\tau$ (ω_c is the cyclotron frequency, and τ the scattering time) in manganites,¹¹ the former contribution to the AMR should be excluded. Though more different from the conventional low-field anisotropic magnetoresistance in ferromagnetic alloys, the AMR effect observed here resembles the ferromagnetic manganite AMR in that it also shows a close relation with JT distortion and MIT, which implies that the spin-orbital coupling may still play an important role behind it. Generally, the spin-orbital coupling is quantified by the Hamiltonian $H_{SO} = \Delta_{SO} \mathbf{L} \cdot \mathbf{S}$, where \mathbf{L} and \mathbf{S} are the orbital and magnetic moments, respectively, and Δ_{SO} is the spin-orbit coupling parameter. For $T > T_{CO}$, the SCMO exhibits little JT distortion and the orbital angular momentum of t_{2g}^3 and e_g^1 configuration is completed quenched by the crystal field, i.e., $\mathbf{L} = 0$, thus no spin-orbit coupling.¹⁵ The collective JT distortion of the MnO_6 octahedron accompanied with the COO formation leads to an unquenching of the $3d$ orbitals, thus the appearance of spin-orbital coupling effects.^{13,15} The evolution of collective JT distortion with decreasing temperatures could result in an increase of AMR below T_{CO} . Meanwhile, the decrease of the AMR could be further ascribed to the suppression of JT distortion at field-induced MIT, which has also been observed in $\text{La}_{0.69}\text{Ca}_{0.31}\text{MnO}_3$ samples.⁸ However, the crossover in AMR is a rather intriguing phenomenon and may be a much more complex process.

In the microscopic theory of AMR for ferromagnets,^{3,4} the sign and the magnitude of AMR can be described by the formula: $(\rho_{\parallel} - \rho_{\perp}) / \rho_{av} = \gamma(\alpha - 1)$, where γ is a spin-orbit coupling constant, α is the ratio between spin \uparrow and spin \downarrow

resistivities, $\alpha = \rho_{\uparrow} / \rho_{\downarrow}$. The positive AMR is generally regarded as a consequence of scattering of majority-spin (spin \uparrow) electrons, while the minority-spin (spin \downarrow) electrons are responsible for the negative AMR. Thus, the crossover in AMR may indicate that magnetic-destruction of the COO state results in severe changes in the electronic structure and a reversal in the spin polarization of dominating conductive electrons, footprint of which has also been found in $\text{La}_{0.95}\text{Ag}_{0.05}\text{MnO}_3$ films.⁶ In addition, the essential larger AMR magnitude in $\rho_{0\bar{1}1}$ than that in ρ_{100} could indicate the stronger spin-orbit coupling along the $[0\bar{1}1]$ direction than that along $[100]$, which is consistent with the huger decrease in $\rho_{0\bar{1}1}$ under magnetic field ($\mu_0 H > 10$ T) and the results in $\text{La}_{2/3}\text{Ca}_{1/3}\text{MnO}_3$ films.⁹ On the other hand, the AMR crossover could also be triggered by the reconstruction of orbital occupation accompanying the magnetic-field-induced MIT, which may be the case for the sign change in ultrathin $\text{Pr}_{0.67}\text{Sr}_{0.33}\text{MnO}_3$ (Ref. 10) and $\text{La}_{0.65}\text{Ca}_{0.35}\text{MnO}_3$ (Ref. 5) films. However, further investigations are needed to reveal the mechanism underlying the AMR crossover.

In summary, the AMR results exhibit a dramatic modification with temperature and magnetic field in charge-orbital-ordered SCMO films. In particular, crossovers in AMR are observed due to the magnetic-destruction of charge/orbital ordering, which indicates a possible severe modification of the SCMO electronic structure or possible orbital reconstruction with the magnetic-field-induced MIT.

This work has been supported by the National Natural Science Foundation of China, the National Basic Research of China, and the Knowledge Innovation Project of the Chinese Academy of Sciences.

¹E. Dagotto and Y. Tokura, *MRS Bull.* **33** 1037 (2008).

²S. Cox, J. Singleton, R. D. McDonald, A. Migliori, and P. B. Littlewood, *Nature Mater.* **7**, 25 (2008).

³T. R. McGuire and R. I. Potter, *IEEE Trans. Magn.* **11**, 1018 (1975).

⁴I. A. Campbell and A. Fert, in *Ferromagnetic Materials*, edited by E. P. Wohlfarth (North-Holland, Amsterdam, 1982), Vol. 3, p. 747.

⁵M. Egilmez, M. M. Saber, A. I. Mansour, R. Ma, K. H. Chow, and J. Jung, *Appl. Phys. Lett.* **93**, 182505 (2008).

⁶I. C. Infante, V. Laukhin, F. Sanchez, J. Fontcuberta, O. Melnikov, O.Y. Gorbenko, and A. R. Kaul, *J. Appl. Phys.* **99**, 08C502 (2006).

⁷J.-B. Yau, X. Hong, A. Posadas, C. H. Ahn, W. Gao, E. Altman, Y. Bason, L. Klein, M. Sidorov, and Z. Krivokapic, *J. Appl. Phys.* **102**, 103901 (2007).

⁸R. W. Li, H. B. Wang, X. W. Wang, X. Z. Yu, Y. Matsui, Z. H. Cheng, B. G. Shen, E. W. Plummer, and J. D. Zhang, *Proc. Natl. Acad. Sci. U.S.A.* **106**, 14224 (2009).

⁹M. Bibes, V. Laukhin, S. Valencia, B. Martínez, J. Fontcuberta, O. Yu Gorbenko, A. R. Kaul, and J. L. Martínez, *J. Phys.: Condens. Matter* **17**, 2733 (2005).

¹⁰Q. Li, H. S. Wang, Y. F. Hu, and E. Wertz, *J. Appl. Phys.* **87**, 5573 (2000).

¹¹J. O'Donnell, J. N. Eckstein, and M. S. Rzchowski, *Appl. Phys. Lett.* **76**, 218 (2000).

¹²Z. Fang, I. V. Solovyev, and K. Terakura, *Phys. Rev. Lett.* **84**, 3169 (2000).

¹³C. Aruta, G. Ghiringhelli, V. Bisogni, L. Braicovich, N. B. Brookes, A. Tebano, and G. Balestrino, *Phys. Rev. B* **80**, 014431 (2009).

¹⁴Y. Z. Chen, J. R. Sun, J. L. Zhao, J. Wang, B. G. Shen, and N. Pryds, *J. Phys. Condens. Matter* (to be published).

¹⁵J. H. Song, J.-H. Park, J.-Y. Kim, B.-G. Park, Y. H. Jeong, H.-J. Noh, S.-J. Oh, H.-J. Lin, and C. T. Chen, *Phys. Rev. B* **72**, 060405(R) (2005).